processes

MDPI

*Article*

# An Experimental Study on Mud Adhesion Performance of a PDC Drill Bit Based on a Biomimetic Non-Smooth Surface

**Ming Chen [1,*] and Qingchao Li [2]**

[1] Drilling Technology Research Institute, Sinopec Oilfield Service Shengli Corporation, Dongying 257000, China
[2] School of Energy Science and Engineering, Henan Polytechnic University, Jiaozuo 454000, China; liqingchao2020@hpu.edu.cn
* Correspondence: mingchen_2012@163.com

**Abstract:** In recent years, polycrystalline diamond compact (PDC) drill bits have seen significant advancements. They have replaced over 90% of the workload traditionally handled by roller cone bits and have become the predominant choice in energy drilling due to their superior efficiency and durability. However, PDC drill bits are susceptible to adhesion of rock cuttings during drilling in muddy formations, leading to mud accumulation on the bit surface. This phenomenon can cause drill bit failure and may contribute to downhole complications, including tool failure and borehole instability. The adhesion issue between PDC drill bits and mud rock cuttings underground is primarily influenced by the normal adhesion force between the drill bit surface and the mud rock cuttings. Therefore, biological non-smooth surface technology is applied to the prevention and control of drill bit balling. It is an optimal selection of biomimetic non-smooth surface structures with reduced adhesion and detachment properties. A non-smooth surface model for the PDC drill bit body is established through the analysis of the morphological characteristics of natural biological non-smooth surfaces. An experimental platform is designed and manufactured to evaluate the adhesion performance of non-smooth surface specimens. Indoor experiments are conducted to test the normal adhesion force of non-smooth surface specimens under varying morphologies, sizes, and contact times with clay. Finally, the anti-adhesion performance of the non-smooth surface unit structures is then analyzed. The normal adhesion force with a contact time of 12 h is as follows: 340 Pa of big square raised, 250 Pa of middle square raised, 190 Pa of small square raised, 315 Pa of big circular groove, 280 Pa of middle circular groove, 200 Pa of small circular groove, 225 Pa of big dot pit, 205 Pa of middle dot pit, and 130 Pa of small dot pit. Compared with the normal adhesion force of 550 Pa for smooth surface specimens with a contact time of 12 h, the anti-adhesion properties of the three non-smooth surface unit structure specimens designed in this paper were verified. We analyzed the anti-adhesion performance of non-smooth surface unit structures. At the critical contact time when the adhesion force tends to stabilize, the adhesion forces of different specimens are as follows: 330 Pa of big square raised, 237.5 Pa of middle square raised, 175 Pa of small square raised, 290 Pa of big circular groove, 250 Pa of middle circular groove, 160 Pa of small circular groove, 210 Pa of big dot pit, 185 Pa of middle dot pit, and 115 Pa of small dot pit. The results indicate that the anti-adhesion effect of small dot pit structures is the most effective, while the anti-adhesion effect of large square convex structures is the least effective. As the size of the unit structure decreases, it becomes more similar to the surface size of the organism. Additionally, a shorter contact time with clay leads to a better anti-adhesion effect. These findings provide new insights and research directions for the effective prevention and control of mud wrapping on PDC drill bits.

check for updates

Academic Editor: Qingbang Meng

Received: 23 April 2025
Revised: 8 May 2025
Accepted: 9 May 2025
Published: 10 May 2025

**Citation:** Chen, M.; Li, Q. An Experimental Study on Mud Adhesion Performance of a PDC Drill Bit Based on a Biomimetic Non-Smooth Surface. *Processes* **2025**, *13*, 1464. https://doi.org/10.3390/pr13051464

**Copyright:** © 2025 by the authors. Licensee MDPI, Basel, Switzerland. This article is an open access article distributed under the terms and conditions of the Creative Commons Attribution (CC BY) license (https://creativecommons.org/licenses/by/4.0/).

**Keywords:** PDC drill bit; non-smooth surface; bit balling; prevention and control; adhesion

## 1. Introduction

Due to the high drilling speed, efficiency, and long service life, PDC drill bits have replaced over 90% of the workload of traditional cone bits, establishing themselves as the primary choice in energy drilling operations. However, in soft formations, PDC drill bits are prone to significant mud wrapping, which can adversely affect drilling performance. This is primarily attributed to the high drilling speed of PDC drill bits in soft formations, which leads to the production of excessive rock cuttings. If rock cuttings are not removed from the well bottom on time, they accumulate in the confined space, increasing the normal adhesion force between the drill bit surface and the cuttings. This leads to nozzle and flow channel blockage, reduces the rock-breaking efficiency of the cutting teeth, and ultimately prevents effective rock cutting, resulting in drill bit mud accumulation (bit balling) [1–3]. The bit balling of the drill bit greatly reduces the drilling ability of the drill bit, causes the cutting teeth to lose their cooling effect, accelerates the wear rate of the drill teeth, reduces the drilling speed, and shortens the service life of the drill bit [4–7]. When the bit balling problem is severe, the drill bit completely loses its drilling ability and needs to be replaced, which will significantly reduce drilling efficiency and increase drilling costs. Scholars have conducted research on the problem of PDC drill bit balling. The Houston Company has set up debris eyebrows on the side of the front end of the blade and developed a bit balling prevention drill bit that can solve the problem of nascent mud bags. In addition, nitriding treatment was also carried out on the surface material of the drill bit, where the positive potential was converted into a strong negative potential, making the drill bit effective in preventing mud entrapment [8]. The dual potassium salt polymer drilling fluid has been developed in the Changqing Oilfield and successfully tested on site in wells GP 12-6 and SHT2, solving the problem of PDC bit mud pack [9,10]. But, the above research solutions are temporary, and the problem of bit balling remains the main problem faced by PDC drill bits.

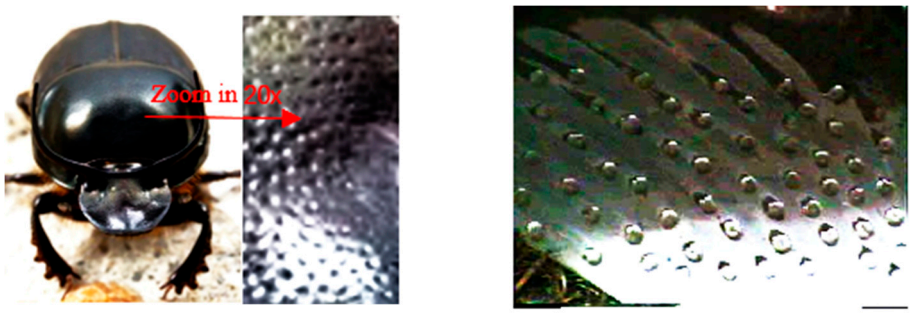
Biomimetics is a new branch of science, and the theory of bionic non-smooth surfaces is applicable to various relative motion interfaces. In the process of long-term evolution and natural selection, organisms retain and develop excellent morphological structures and surface properties, providing a natural blueprint for humans as biomimetic objects. Non-smooth surfaces have the function of reducing adhesion, detachment, and resistance under sticky and wet conditions [11,12]. When seeking methods to prevent adhesion and reduce friction, scholars have found that many flying organisms, aquatic organisms, and some organisms living in soil have the lowest resistance and adhesion force on non-smooth surfaces, rather than smooth surfaces [13–15]. Scholars at home and abroad have conducted preliminary research on the application of biomimetic drill bits in bit balling prevention and control and have achieved some results. The former Soviet Union officially applied bionics to drilling and developed a double drill bit that imitated the teeth of ancient dinosaurs, increasing drilling speed by nearly twice [16]. Jilin University has developed PDC biomimetic drill bits based on biomimetic non-smooth surfaces. Compared with ordinary drill bits [17], biomimetic non-smooth surface morphology drill bits have the characteristics of high efficiency, wear resistance, and better drilling effect during rock breaking. However, the lifespan of the newly developed drill bits mentioned above is not long, which limits their practical application in production.

This article focuses on the prevention and control of drill bit balling and applies the non-smooth geometric surface morphology from bionics to the design of PDC drill bit

surface structure. A non-smooth surface anti-adhesion performance experimental bench is designed and processed. Through indoor experimental methods, the normal adhesion force between specimens and clay under different non-smooth surface morphologies, sizes, and contact time states is measured to study the anti-adhesion performance of non-smooth surface unit structure, providing a certain foundation for the research of PDC drill bit mud pocket prevention and control.

## 2. Materials and Methods

There are two types of surfaces for living organisms: non-smooth and smooth. From a biomimetic perspective, the adaptability of biological surfaces to the natural environment is the best result obtained through long-term natural selection in the natural environment [4,18]. For example, a biomimetic plow mimics the non-smooth surface of animal dots and pits in the soil, using the back plate of the beetle's chest as a template, as shown in Figure 1. A non-smooth surface with circular pits can change the direction of force at the front end of the soil, generate normal micro vibrations, reduce tangential adhesion force, reduce water film tension, and exhibit excellent non-clay properties in practical applications, greatly reducing resistance on the plow wall and improving the lifespan of the plow [19,20].




(**a**) Dung beetle front chest back plate (**b**) Biomimetic plow for agriculture

**Figure 1.** Biomimetic plow using the dung beetle's front chest back plate as a template.

The non-smooth surface shapes of organisms include grooves, pits, protrusions, wavy plates, and scales [21,22]. The complete system related to biomimetics in drilling has not yet been formed, and the application of biomimetics to the field of drilling is still in the exploratory stage. This article mainly focuses on the study of the non-smooth surface morphology of PDC drill bits for the prevention and control of bit balling [23–25]. Taking several typical animal body surfaces on land and in the sea as examples, we analyze their non-smooth surface morphology and size. Table 1 shows several typical non-smooth surfaces with anti-adhesion properties.

**Table 1.** Typical anti-adhesion properties of non-smooth surfaces.

| Biological Name | Conch with Convex Plate | Tooth | Oysters | Dung Beetle Chest and Back Plate | Turbo Cornulus | Spiny Snail |
|---|---|---|---|---|---|---|
| Surface morphology | Protrusion | Protrusion | Pit | Pit | Unevenness | Groove |
| Distribution status | Approximately spherical | Uniformly distributed | Randomly distributed | Uniformly distributed | Randomly distributed | Uniformly distributed |

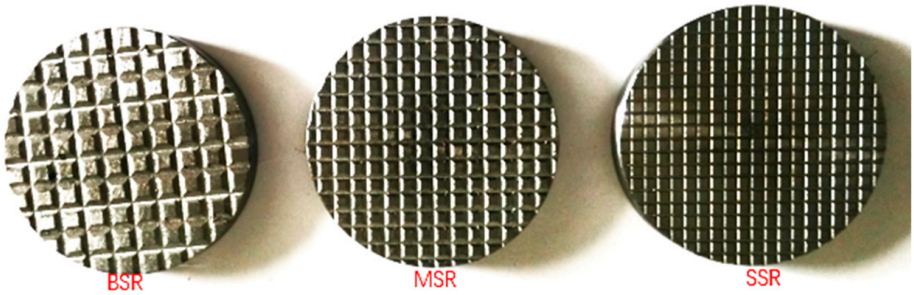
The non-smooth surface morphology design of PDC drill bits should be based on objective conditions, such as the strength and hardness of the drill bit material itself, the

difference between the strength and hardness of the biological prototype material, and the difficulty of industrial processing, combined with the size [26], shape [27], and density of the biological prototype [28–30]. Therefore, the design principle of the non-smooth surface unit structure is that the shape and size of the specimen are close to or similar to the biological prototype specimen, and the distribution is uniform [31–33]. All specimens have a uniform outer dimension, with a diameter of 80 mm and a height of 12 mm. At present, mechanical processing is difficult to meet the requirements at the micrometer level. Considering the process parameters of the PDC drill bit body, mechanical processing conditions, and the morphological similarity of protrusions, grooves, and pits, the structural parameters of the non-smooth surface unit body are finally selected, as shown in Table 2.

**Table 2.** Structural parameters of non-smooth surface specimens.

| Morphology | Specimen Name | Unit Structure Dimensions/mm |
|---|---|---|
| Square Raised | Small Square Raised (SSR) | Side length 1, height 0.5, spacing 1 |
| | Middle Square Raised (MSR) | Side length 2, height 1, spacing 2 |
| | Big Square Raised (BSR) | Side length 3, height 1.5, spacing 3 |
| Circular Groove | Small Circular Groove (SCG) | Slot depth 0.5, width 1, spacing 1 |
| | Middle Circular Groove (MCG) | Slot depth 1, width 2, spacing 2 |
| | Big Circular Groove (BCG) | Slot depth 1.5, width 3, spacing 3 |
| Dot Pit | Small Dot Pit (SDP) | Diameter 1, depth 0.5, spacing 1 |
| | Middle Dot Pit (MDP) | Diameter 2, depth 1, spacing 2 |
| | Big Dot Pit (BDP) | Diameter 3, depth 1.5, spacing 3 |
| Smoothness Surface | SS | / |

According to the parameters of the specimens in Table 2, a total of 10 specimens were processed, and the actual objects are shown in Figure 2.

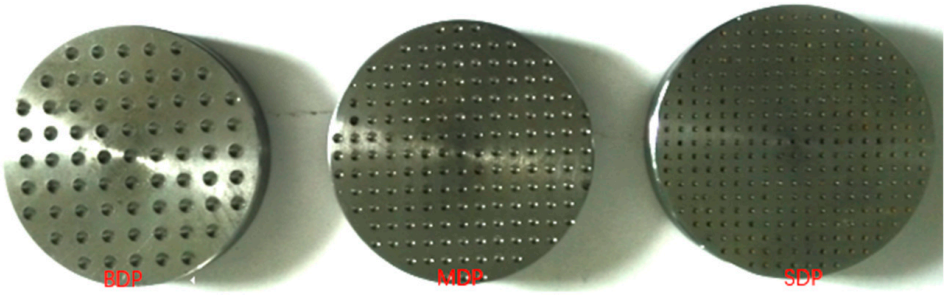



(**a**) Square raised specimen

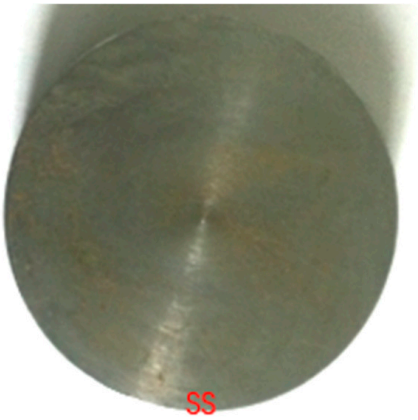



(**b**) Circular groove specimen

**Figure 2.** *Cont.*




(**c**) Dot pit specimens




(**d**) Smooth surface specimen

**Figure 2.** Physical object of the experimental specimen.

## 3. Results

### *3.1. Experimental Bench*

The experimental bench includes a clay container, a structural fixing bench, a tension sensor, and a tension display instrument [34,35]. Its main function is to measure the adhesion force between the specimen and the clay. To reduce the influence of boundary effects, it is required that the area of the clay container be more than 10 times the plane area of the specimen [36]. To ensure consistency in the depth of the specimen sinking into the clay during the experiment, a certain length of the support rod is fixed in the center of the clay container to support the specimen, preventing it from sinking too deep and avoiding excessive adhesion of clay to the periphery of the specimen, which may affect the experimental results. The structural fixing platform requires the platform to be fixed together with the clay container, ensuring that the suspension point of the tension sensor is on the same vertical line as the center of the container [37–39]. At the same time, the platform must have a certain strength and height to ensure the strength and space for the tension sensor to be lifted up and down. The tension sensor and tension display instrument should be sensitive enough to accurately record the maximum tension generated during the measurement process, including the maximum adhesion force between the specimen and clay [40]. The schematic diagram and physical object of the experimental bench design are shown in Figure 3.

During the experiment, fix the bench on a horizontal plane. The tension sensor has the function of storing peak values. The platform and tension sensor are used together to ensure that the normal tension is always present [41–43]. To restore the mud environment of downhole drill bits, the container should have the function of holding saturated clay. Through this experimental platform, different normal adhesion forces can be measured.

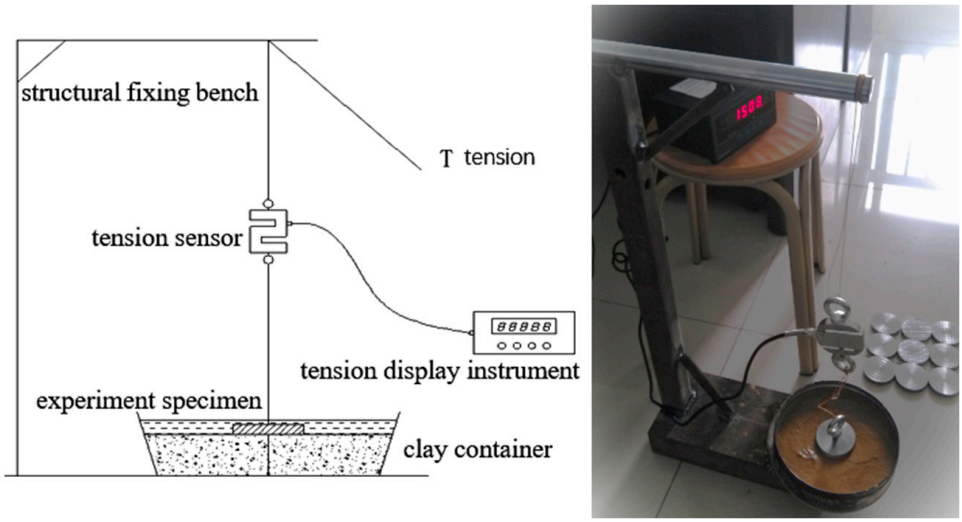



**Figure 3.** Experimental bench design diagram and physical object.

### *3.2. Anti-Adhesion Experiment*

According to the parameters in Table 2, non-smooth surface unit structures of different sizes and shapes are uniformly distributed on the surface of the formed 45# steel metal specimens. Contact different specimens with saturated clay, measure the adhesion force between specimens and clay under different contact time states, and then analyze the influence of the morphology, size, and contact time with clay of biomimetic non-smooth surface units on the adhesion force [44–46]. To ensure the accuracy of the experiment, the clay was air dried, ground, and then placed separately in a container. The composition of clay is shown in Table 3. To simulate the working state of the downhole drill bit and saturate the clay, let it stand for 72 h to ensure uniform contact between water and soil particles. Put the processed saturated clay into a container and compact the surface of the clay to make it smooth. Adjust the tension sensor to ensure a good fit with the platform, connect the tension sensor to the specimen, and lift the specimen to a certain height above the clay using the tension sensor [47–49]. When lowering, ensure that the contact surface between the specimen and the clay is a horizontal plane so that the measurement result is the normal adhesion force between the clay and the specimen interface. The displacement speed is controlled to increase to 0.005 m/s, and the displacement speed is lowered to 0.01 m/s. The contact time between each specimen and clay is 20 min, 40 min, 1 h, 1.5 h, 2 h, 2.5 h, 3 h, 3.5 h, 4 h, 4.5 h, 5 h, 5.5 h, 6 h, 6.5 h, 7 h, 7.5 h, 8 h, 8.5 h, 9 h, 9.5 h, 10 h, 10.5 h, 11 h, 11.5 h, and 12 h.

**Table 3.** Composition of clay.

| Composition | Quartz | Calcite | Pyrite | Kaolinite | Montmorillonite | Illite | Others |
|---|---|---|---|---|---|---|---|
| Content (%) | 9.39 | 1.55 | 0.8 | 36.52 | 34.31 | 17.13 | 0.3 |

Under identical experimental steps and conditions, 10 specimens were tested sequentially. First, perform the lowering action to ensure that the load is applied without damaging the saturated clay. The specimen is in horizontal contact with the central support rod of the container under its own gravity [49]. Conduct the experiment according to the set contact time. Once the set contact time is reached, immediately perform the lifting action, paying attention to maintaining a slow and constant speed [50,51]. After the instrument completes the lifting action, read the tension F between the specimen and the clay from the tension display and calculate the adhesion force through the equation $P = F/A$, where $A$

denotes the projected area of the specimen in the vertical direction of the applied tensile force. Each specimen needs to be measured at different contact times; so, for each measurement, the specimen needs to be wiped clean, sun dried, and the saturated clay needs to be re-leveled [52–54]. Measure the normal adhesion force between specimens and clay under different non-smooth surface morphologies, sizes, and contact times. To reduce errors, three experiments were conducted at each contact time, and the average value was taken as the normal adhesion force experiment value for that contact time.

## 4. Analysis

The factors affecting the adhesion of biomimetic non-smooth surface specimens include the morphology, size, and contact time with clay of the non-smooth surface unit [55–57]. Select non-smooth surface specimens as the research object, test the normal adhesion force of non-smooth surface specimens under different shapes, sizes, and contact times, and analyze the effect of three factors on the normal adhesion force at the interface between clay and specimens [58]. The experimental results are shown in Figures 4–6.

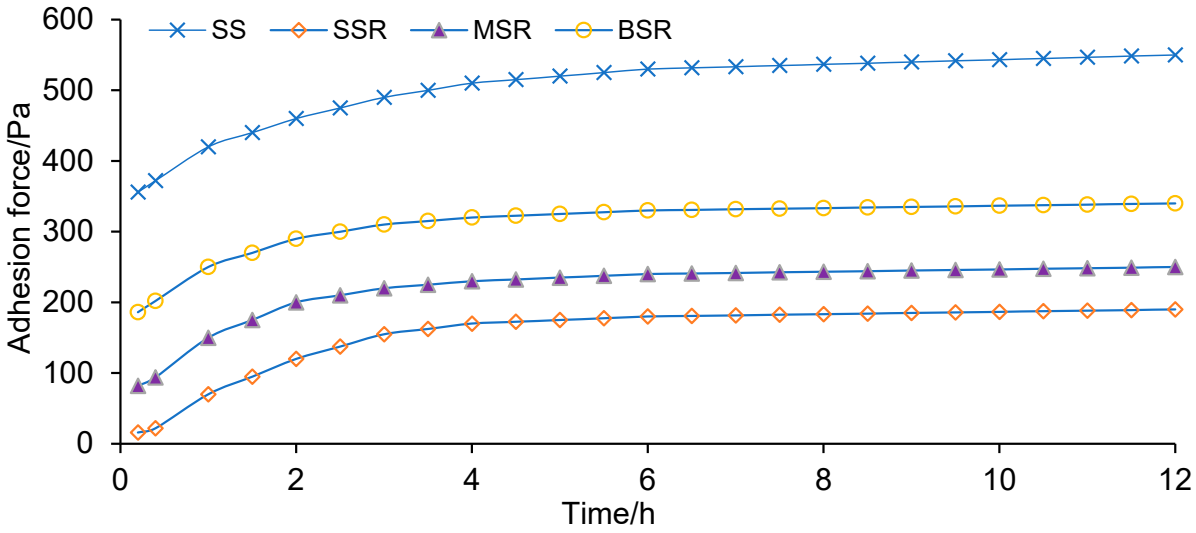



**Figure 4.** Adhesion force of the square raised specimens.

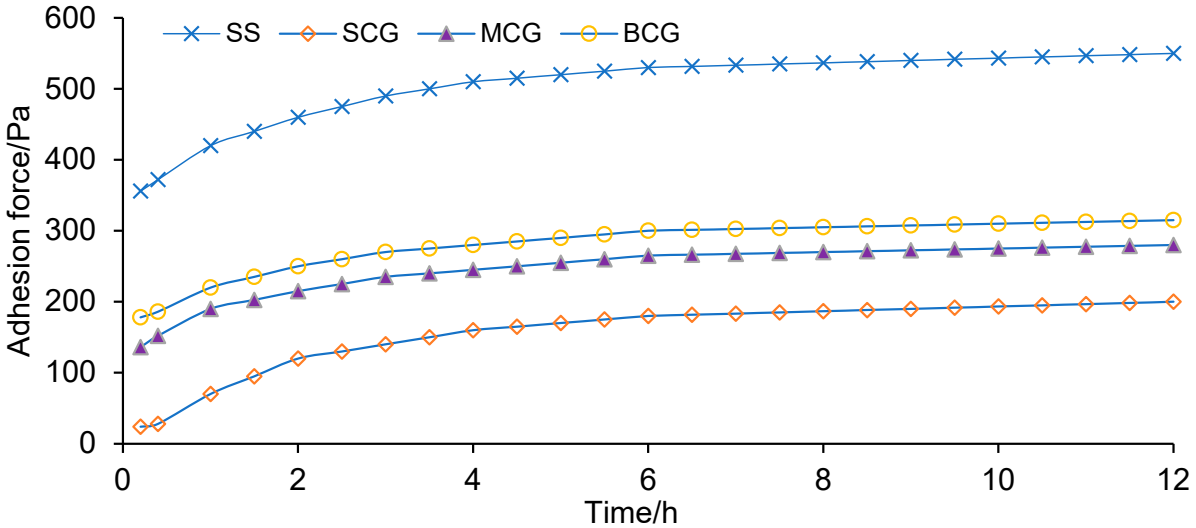



**Figure 5.** Adhesion force of the circular groove specimens.

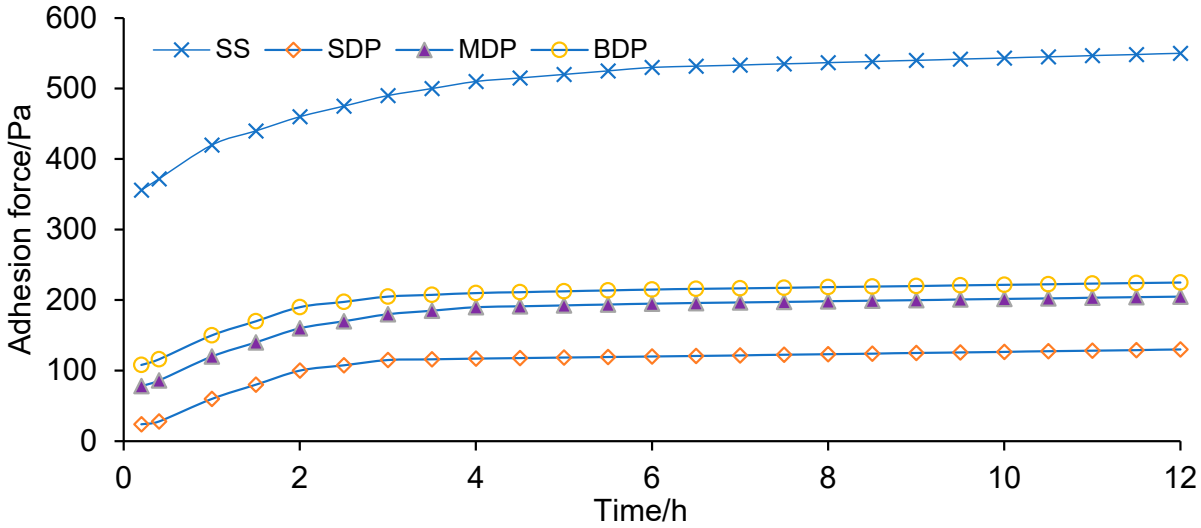



**Figure 6.** Adhesion force of the dot pit specimens.

To increase contrast, the normal adhesion force of smooth surface specimens was tested. By comparing the normal adhesion forces of the 12 h specimens in Table 4, the normal adhesion forces of the circular groove specimen, square convex specimen, and circular concave specimen are generally smaller than those of the smooth plane specimen, indicating that the three non-smooth surface unit structures established through biomimetic analysis have anti-adhesion functions [59,60].

**Table 4.** Normal adhesion force with a contact time of 12 h.

| Specimen Name | BSR | MSR | SMR | BCG | MCG | SCG | BDP | MDP | SDP |
|---|---|---|---|---|---|---|---|---|---|
| Normal adhesion force/Pa | 340 | 250 | 190 | 315 | 280 | 200 | 225 | 205 | 130 |

(1) The influence of the morphology of non-smooth surface unit structures on adhesion performance is compared. The adhesion force generated by three types of non-smooth surface unit structures is the smallest in the normal direction for small dot pit specimens and the largest in the normal direction for big square raised specimens [61]. Therefore, it can be concluded that the anti-adhesion effect of the three types of non-smooth surface unit structures is the best for small dot pit specimens, while the anti-adhesion effect is the worst for big square raised specimens.

(2) The influence of non-smooth surface unit size on adhesion performance is examined. The normal adhesion force generated by three types of non-smooth surface unit structures increases with the increase in unit size, and the smaller the unit structure size, the closer it is to the surface size of the organism, and the better the anti-adhesion effect. Under the allowable processing conditions and material properties, the structural dimensions of non-smooth surface units should be as close as possible to the surface dimensions of the organism.

(3) The influence of contact time between specimens and clay on adhesion performance is examined. The normal adhesion force between specimens and clay in three types of non-smooth surface unit structure specimens increases with increasing contact time. When the contact time reaches the critical contact time, as shown in Table 5, the adhesion force tends to stabilize. The critical contact time of smooth surface specimens is 9 h, and the adhesion force is 540 Pa. All non-smooth surface specimens did not reach this adhesion force value during the test contact time, further verifying that non-smooth surfaces have anti-adhesion performance.

**Table 5.** Critical contact time for the adhesion force to stabilize.

| Specimen Name | BSR | MSR | SMR | BCG | MCG | SCG | BDP | MDP | SDP |
|---|---|---|---|---|---|---|---|---|---|
| Critical time | 6 h | 5.5 h | 5 h | 5 h | 4.5 h | 4 h | 4 h | 3.5 h | 3 h |
| Adhesion force/Pa | 330 | 237.5 | 175 | 290 | 250 | 160 | 210 | 185 | 115 |

## 5. Conclusions

This article conducted research on the prevention and control of PDC drill bit mud bags based on non-smooth surfaces. Through experiments, it was preliminarily verified that the application of non-smooth surfaces, such as circular dots and pits, to the surface design of PDC drill bits has anti-adhesion properties. This study did not consider the influence of complex underground environments, such as cutting teeth and nozzles. Further in-depth research will be conducted, and the research results will open up new research directions for the prevention and control of PDC drill bit mud bags. The specific conclusions obtained are as follows:

(1) In response to the problem of bit balling easily formed by PDC drill bits during drilling in muddy formations, the non-smooth surface morphology in biomimetics is applied to the surface structure design of PDC drill bits. The morphology, size, and arrangement of the non-smooth surface unit units of living organisms are analyzed, and a non-smooth surface unit structure specimen with a certain anti-adhesion function is designed.

(2) Design an experimental bench and use indoor experimental methods to test the normal adhesion force of non-smooth surface specimens under different morphologies, sizes, and contact times. The normal adhesion force with a contact time of 12 h is as follows: 340 Pa of big square raised, 250 Pa of middle square raised, 190 Pa of small square raised, 315 Pa of big circular groove, 280 Pa of middle circular groove, 200 Pa of small circular groove, 225 Pa of big dot pit, 205 Pa of middle dot pit, and 130 Pa of small dot pit. Compared with the normal adhesion force of 550 Pa for smooth surface specimens with a contact time of 12 h, the anti-adhesion properties of the three non-smooth surface unit structure specimens designed in this paper were verified to have anti-adhesion properties.

(3) Analyze the influence of three factors: non-smooth surface morphology, size, and contact time with clay on the magnitude of adhesion force. At the critical contact time when the adhesion force tends to stabilize, the adhesion forces of different specimens are as follows: 330 Pa of big square raised, 237.5 Pa of middle square raised, 175 Pa of small square raised, 290 Pa of big circular groove, 250 Pa of middle circular groove, 160 Pa of small circular groove, 210 Pa of big dot pit, 185 Pa of middle dot pit, and 115 Pa of small dot pit. The results show that the anti-adhesion effect of small dot pit structures is the best, while the anti-adhesion effect of big square raised structures is the worst. The smaller the size of the unit structure, the closer it is to the surface size of the organism, and the shorter the contact time with clay, the better the anti-adhesion effect.

**Author Contributions:** Conceptualization, M.C. and Q.L.; methodology, M.C.; software, M.C.; validation, M.C. and Q.L.; formal analysis, Q.L.; investigation, M.C.; resources, M.C.; data curation, M.C.; writing—original draft preparation, M.C.; writing—review and editing, M.C.; visualization, M.C.; supervision, M.C.; project administration, M.C.; funding acquisition, Q.L. All authors have read and agreed to the published version of the manuscript.

**Funding:** The current paper was sponsored by the National Key R&D Program Project (Government Key Special Project) (2021YFE0111400), the Key Research Platform Fund Special Project of National Engineering Laboratory for Marine Geophysical Exploration and Exploration Equipment (20CX02319A), and the Ministry of Education Industry University Cooperation Collaborative Education Project (220506517103435).

**Data Availability Statement:** The original contributions presented in this study are included in the article. Further inquiries can be directed to the corresponding authors.

**Acknowledgments:** The authors would like to express their deep gratitude for the invaluable support of these institutions. Likewise, the authors express their appreciation for the comments of the anonymous reviewers and the editor, who have considerably improved this article.

**Conflicts of Interest:** Author Chen Ming was employed by the Drilling Technology Research Institute. The remaining authors declare that the research was conducted in the absence of any commercial or financial relationships that could be construed as a potential conflict of interest.

## References

1. Zhang, W.B.; Shi, H.Z.; Xi, C.M.; Zhang, N.; Xiong, C.; Chen, Z. Experimental study on rock cutting with the combination of conical diamond elements and conventional PDC cutters. *China Pet. Mach.* **2023**, *51*, 33–39.
2. Wang, W.; Cheng, Z.Y.; Chen, X.Y.; Xu, Y.; Peng, G. Design and application of pulse cavitation PDC bit. *China Pet. Mach.* **2021**, *49*, 24–30+38.
3. Deng, R.; He, X.J.; Huang, A.L. Experimental study on rock crack characteristics of PDC cutter in the process of rock breaking. *Pet. Drill. Tech.* **2024**, *52*, 38–44.
4. Wen, X.; Liu, G.; Li, J.; Zha, C.; Guo, X. A study of newly compound impactor aiming to mitigate stick-slip vibration on drill bit for deep formations. *Chem. Technol. Fuels Oils* **2025**, *60*, 1668–1675. [CrossRef]
5. Smith, J.R.; Lund, J.B.; Galloway, R.K. Friction on PDC cutters at high normal stress. *J. Energy Resour. Technol.* **2002**, *124*, 146–153. [CrossRef]
6. Detournay, E.; Richard, T.; Shepherd, M. Drilling response of drag bits: Theory and experiment. *Int. J. Rock Mech. Min. Sci.* **2008**, *45*, 1347–1360. [CrossRef]
7. Wang, B.; Li, J.; Zou, D.Y.; Yang, H.; Huang, T. Mechanisms and distribution pattern of abrasions on PDC bits for highly-abrasive hard-rock. *Spec. Oil Gas Reserv.* **2018**, *25*, 149–153.
8. Hu, H.; Guan, Z.; Zhang, B.; Xu, Y.; Liu, Y.; Wang, B. Structured design of weight-on-bit self-adjusting PDC bit based on stress field analysis and experiment evaluation. *J. Pet. Sci. Eng.* **2021**, *196*, 1076–1092. [CrossRef]
9. Liu, X.; Zou, D.; Yu, J.; Cui, Y. Experimental research on the impregnated diamond bit wear model. *Chem. Technol. Fuels Oils* **2023**, *59*, 113–122. [CrossRef]
10. Lei, M.; Sun, J.S.; Zhu, H.Y.; Huang, W.; Cai, Z. Synthesis and characterization of natural rosin-modified silica nanocomposite and its green multifunctional applications for drilling fluid. *Colloids Surf. A Physicochem. Eng. Asp.* **2024**, *702*, 134994. [CrossRef]
11. Li, Q.; Li, Q.; Cao, H.; Wu, J.; Wang, F.; Wang, Y. The Crack Propagation Behaviour of $CO_2$ Fracturing Fluid in Unconventional Low Permeability Reservoirs: Factor Analysis and Mechanism Revelation. *Processes* **2025**, *13*, 159. [CrossRef]
12. Shirvanimoghaddam, K.; Balaji, K.V.; Yadav, R.; Zabihi, O.; Ahmadi, M.; Adetunji, P.; Naebe, M. Balancing the toughness and strength in polypropylene composites. *Compos. Part B Eng.* **2021**, *223*, 109121. [CrossRef]
13. Liu, Y.Z.; Lei, J.Y.; Wang, Z.H. Dynamic response of nacre-like brick and mortar structure under impact load. *Chin. J. High-Press. Phys.* **2022**, *36*, 125–133.
14. Junior, W.K.; Guanabara, A.S. Methodology for product design based on the study of bionics. *Mater. Des.* **2005**, *26*, 149–155. [CrossRef]
15. Li, Q.; Li, Q.; Wu, J.; Li, X.; Li, H.; Cheng, Y. Wellhead stability during development process of hydrate reservoir in the Northern South China Sea: Evolution and mechanism. *Processes* **2025**, *13*, 40. [CrossRef]
16. Cao, P.L.; Gao, K.; Wang, W.L.; Yin, K. Optimization design and testing of stepped impact compaction drill bit structure. *Pet. Mach.* **2009**, *37*, 20–23.
17. Zhang, C.; Yang, X.; Zhu, Z.; Ke, X.; Zhang, Z.; Luo, H.; Ma, Y.; Song, D. Experimental study on shale-breaking of special-shaped cutter PDC bit. *Geomech. Geophys. Geo-Energy Geo-Resour.* **2024**, *10*, 123. [CrossRef]
18. Li, Q.; Wu, J.; Li, Q.; Wang, F.; Cheng, Y. Sediment Instability Caused by Gas Production from Hydrate-Bearing Sediment in Northern South China Sea by Horizontal Wellbore: Sensitivity Analysis. *Nat. Resour. Res.* **2025**, *34*, 1667–1699.
19. Liang, X.; Shan, C.A.; Wang, W.; Li, Z.; Zhu, D.; Xu, J.; Zhang, Z.; Zhang, Z.; Luo, Y.; Yuan, X. Exploration and development in the Zhaotong national shale gas demonstration area: Progress and prospects. *Nat. Gas Ind. B* **2023**, *10*, 44–61. [CrossRef]

20. Li, Q.; Li, Q.; Wang, F.; Wu, J.; Wang, Y. The carrying behavior of water-based fracturing fluid in shale reservoir fractures and molecular dynamics of sand-carrying mechanism. *Processes* **2024**, *12*, 2051. [CrossRef]
21. Liu, W.; Deng, K.; Li, R.; Li, L.; Zhu, X.; Gong, S. The performance and failure mechanism of drill bit in granite formation drilling. *Res. Artic. Pet. Eng.* **2023**, *48*, 9477–9492. [CrossRef]
22. Li, Q.; Li, Q.; Han, Y. A numerical investigation on kick control with the displacement kill method during a well test in a deep-water gas reservoir: A case study. *Processes* **2024**, *12*, 2090. [CrossRef]
23. Wu, Z.; Yuan, R.; Zhang, W.; Liu, J.; Hu, S. Structure design of bionic PDC cutter and the characteristics of rock breaking processes. *Processes* **2023**, *12*, 66. [CrossRef]
24. Qiao, J.; Zhu, L.N.; Yue, W.; Fu, Z.Q.; Kang, J.J.; Wang, C.B. The effect of attributes of micro-shapes of laser surface texture on the wettability of WC-CrCo metal ceramic coatings. *Surf. Coat. Technol.* **2018**, *334*, 429–437. [CrossRef]
25. Kerr, C.J. PDC drill bit design and field application evolution. *J. Pet. Technol.* **1988**, *40*, 327–332. [CrossRef]
26. Yang, Y.; Yang, Y.; Ren, H.; Qi, Q.; Chen, X. Research on the working mechanism of the PDC drill bit in compound drilling. *J. Pet. Sci. Eng.* **2020**, *185*, 106647. [CrossRef]
27. Mazen, A.Z.; Mujtaba, I.M.; Hassanpour, A.; Rahmanian, N. Mathematical modelling of performance and wear prediction of PDC drill bits: Impact of bit profile, bit hydraulic, and rock strength. *J. Pet. Sci. Eng.* **2020**, *188*, 106849. [CrossRef]
28. Taylor, M.R.; Murdock, A.D.; Evans, S.M. High penetration rates and extended bit life through revolutionary hydraulic and mechanical design in PDC drill bit development. *SPE Drill. Complet.* **1999**, *14*, 34–41. [CrossRef]
29. Liu, Y.; Zhou, L.; Wan, X.; Tang, Y.; Liu, Q.; Li, W.; Liao, J. Synthesis and Characterization of a Temperature-Sensitive Microcapsule Gelling Agent for High-Temperature Acid Release. *ACS Omega* **2024**, *9*, 20849–20858. [CrossRef]
30. Pessier, R.; Damschen, M. Hybrid bits offer distinct advantages in selected roller-cone and PDC-bit applications. *SPE Drill. Complet.* **2011**, *26*, 96–103. [CrossRef]
31. Panayirci, H.M. An experimental study on steering response of PDC drill bits. *J. Pet. Sci. Eng.* **2022**, *208*, 109440. [CrossRef]
32. Huang, K.; Ai, Z.; Yang, Y.; Xie, Z. The improved rock breaking efficiency of an annular-groove PDC bit. *J. Pet. Sci. Eng.* **2019**, *172*, 425–435. [CrossRef]
33. Li, Q.; Liu, J.; Wang, S.; Guo, Y.; Han, X.; Li, Q.; Cheng, Y.; Dong, Z.; Li, X.; Zhang, X. Numerical insights into factors affecting collapse behavior of horizontal wellbore in clayey silt hydrate-bearing sediments and the accompanying control strategy. *Ocean Eng.* **2024**, *297*, 117029. [CrossRef]
34. Mao, L.; He, J.; Zhu, J.; Jia, H.; Gan, L. Dynamic characteristic response of PDC bit vibration coupled with drill string dynamics. *Geoenergy Sci. Eng.* **2024**, *233*, 212524. [CrossRef]
35. Bondarenko, A.V.; Islamov, S.R.; Ignatyev, K.V.; Mardashov, D.V. Laboratory studies of polymer compositions for well-kill under increased fracturing. *Perm J. Pet. Min. Eng.* **2020**, *20*, 37–48. [CrossRef]
36. Belousov, A.; Lushpeev, V.; Sokolov, A.; Sultanbekov, R.; Tyan, Y.; Ovchinnikov, E.; Shvets, A.; Bushuev, V.; Islamov, S. Experimental Research of the Possibility of Applying the Hartmann–Sprenger Effect to Regulate the Pressure of Natural Gas in Non-Stationary Conditions. *Processes* **2025**, *13*, 1189. [CrossRef]
37. Li, Q.; Wang, Y.; Wang, F.; Li, Q.; Kobina, F.; Bai, H.; Yuan, L. Effect of a modified silicone as a thickener on rheology of liquid $CO_2$ and its fracturing capacity. *Polymers* **2019**, *11*, 540. [CrossRef]
38. Pryhorovska, T.O.; Chaplinskiy, S.S.; Kudriavtsev, I.O. Finite element modelling of rock mass cutting by cutters for PDC drill bits. *Pet. Explor. Dev.* **2015**, *42*, 888–892. [CrossRef]
39. Liu, C.; Zheng, X.; Wang, G.; Xu, M.; Li, Z. Research on drilling response characteristics of two-wing PDC bit. *Sustainability* **2020**, *12*, 406. [CrossRef]
40. Abbas, R.K. A review on the wear of oil drill bits (conventional and the state of the art approaches for wear reduction and quantification). *Eng. Fail. Anal.* **2018**, *90*, 554–584. [CrossRef]
41. Zhang, J.; Cui, M.; Wang, Q.; Ren, H.; Ji, G.; Shao, F.; Zhuo, L.; Li, H.; Yu, J. Experimental study on rock drilling vibration of PDC bit in interbedded formations. *Geoenergy Sci. Eng.* **2025**, *244*, 213452. [CrossRef]
42. Wang, Z.; Wang, C.; Feng, S.; Li, N.; Zhang, Z.; Fan, Y. Mechanism and Experimental Research on Rock Breaking by Cutting Teeth of High-Speed PDC Drill Bit. *Processes* **2025**, *13*, 1213. [CrossRef]
43. Zhang, C.; Zhao, Y.; Gao, K.; Zhang, C.; Lv, X.; Xie, X. Simulation and experimental investigations of ultrasonic-assisted drilling with Micro-PDC bit. *Geoenergy Sci. Eng.* **2023**, *223*, 211480. [CrossRef]
44. Motahhari, H.R.; Hareland, G.; James, J.A. Improved drilling efficiency technique using integrated PDM and PDC bit parameters. *J. Can. Pet. Technol.* **2010**, *49*, 45–52. [CrossRef]
45. Kuang, Y.; Zhang, M.; Feng, M.; Zhang, Y.; Han, Y.; Peng, Y. Simulation and experimental research of PDC bit cutting rock. *J. Fail. Anal. Prev.* **2016**, *16*, 1101–1107. [CrossRef]
46. Ersoy, A.; Waller, M.D. Drilling detritus and the operating parameters of thermally stable PDC core bits. *Int. J. Rock Mech. Min. Sci.* **1997**, *34*, 1109–1123. [CrossRef]

47. Tu, J.; Wang, X.; Dai, W.; Zhang, H.; Liu, B. Performance improvement of PDC and PDC bits by cryogenic treatment. *Geoenergy Sci. Eng.* **2023**, *221*, 211350. [CrossRef]
48. Gao, K.; Xu, X.; Jiao, S.; Li, Z. Modeling and experimental research on temperature field of full-sized PDC bits in rock drilling and coring. *Energy Rep.* **2022**, *8*, 8928–8938. [CrossRef]
49. Huang, K.; Yang, Y.; Li, G.; Wang, Y.; Ren, H.; Niu, S. Torsion and vibration reduction mechanism of roller PDC hybrid bit. *J. Pet. Sci. Eng.* **2022**, *208*, 109491. [CrossRef]
50. Black, A.D.; Walker, B.H.; Tibbitts, G.A.; Sandstrom, J.L. PDC bit performance for rotary, mud motor, and turbine drilling applications. *SPE Drill. Eng.* **1986**, *1*, 409–416. [CrossRef]
51. Tian, K.; Detournay, E. Influence of PDC bit cutter layout on stick–slip vibrations of deep drilling systems. *J. Pet. Sci. Eng.* **2021**, *206*, 109005. [CrossRef]
52. Taylor, S.; Besson, A.; Minto, D.; Mampuk, I.S. Unique PDC bit technologies combine to reduce drilling time in interbedded formations. *SPE Drill. Complet.* **2000**, *15*, 112–117. [CrossRef]
53. Chen, P.; Miska, S.; Yu, M.; Ozbayoglu, E. Modeling of cutting rock: From PDC cutter to PDC bit—Modeling of PDC bit. *SPE J.* **2021**, *26*, 3465–3487. [CrossRef]
54. Liao, Q.; Cui, G.; Xie, T.; Li, H.; Zhang, L.; Wang, Y. Study on Different Kinds of Drill Bits and Their Usage in Hard-to-Drill Formations. *Chem. Technol. Fuels Oils* **2023**, *59*, 783–790. [CrossRef]
55. Li, Q.; Cheng, Y.; Li, Q.; Zhang, C.; Ansari, U.; Song, B. Establishment and evaluation of strength criterion for clayey silt hydrate-bearing sediments. *Energy Sources Part A Recovery Util. Environ. Eff.* **2018**, *40*, 742–750. [CrossRef]
56. Huang, K.; Zhou, C.; Yang, Y.; Ren, H.; Niu, Q. Working Load Characteristics of the PDC-Cone Composite Bit under Impact and Scraping. *Shock Vib.* **2020**, *2020*, 7540519. [CrossRef]
57. Ozturk, O.M.; Kilic, Z.M.; Altintas, Y. Mechanics and dynamics of orbital drilling operations. *Int. J. Mach. Tools Manuf.* **2018**, *129*, 37–47. [CrossRef]
58. Li, Q.; Wang, Y.; Wang, Y.; San, J.; Li, Q.; Foster, G. Synthetic process on hydroxyl-containing polydimethylsiloxane as a thickener in $CO_2$ fracturing and thickening performance test. *Energy Sources Part A Recovery Util. Environ. Eff.* **2018**, *40*, 1137–1143. [CrossRef]
59. Wang, Q.; Zhang, D.; Tang, K.; Zhang, Y. A mechanics based prediction model for tool wear and power consumption in drilling operations and its applications. *J. Clean. Prod.* **2019**, *234*, 171–184. [CrossRef]
60. Chen, X.; Gao, D.; Guo, B.; Feng, Y. Real-time optimization of drilling parameters based on mechanical specific energy for rotating drilling with positive displacement motor in the hard formation. *J. Nat. Gas Sci. Eng.* **2016**, *35*, 686–694. [CrossRef]
61. Liu, Y.; Zhou, L.; Tang, Y.; Liu, Q.; Li, W.; Zhang, Y. Synthesis and Characterization of a Resin/Acrylamide-2-acrylamide-2-methylpropane Sulfonate-Diallyl Dimethyl Ammonium Chloride-N-vinyl-2-pyrrolidinone Polymer Microcapsule Gelling Agent for Oil and Gas Field Transformation. *ACS Omega* **2023**, *8*, 49080–49087. [CrossRef] [PubMed]


**Disclaimer/Publisher's Note:** The statements, opinions and data contained in all publications are solely those of the individual author(s) and contributor(s) and not of MDPI and/or the editor(s). MDPI and/or the editor(s) disclaim responsibility for any injury to people or property resulting from any ideas, methods, instructions or products referred to in the content.